IMECE2004-59621

E. COLI INSPIRED PROPULSION FOR SWIMMING MICROROBOTS

Bahareh Behkam
Mechanical Engineering Department
Carnegie Mellon University
Pittsburgh, PA 15213
bbehkam@andrew.cmu.edu

Metin Sitti
Mechanical Engineering Department and Robotics Institute
Carnegie Mellon University
Pittsburgh, PA 15213
sitti@cmu.edu

ABSTRACT

Medical applications are among the most fascinating areas of microrobotics. For long, scientists have dreamed of miniature smart devices that can travel inside the human body and carry out a host of complex operations such as minimally invasive surgery (MIS), highly localized drug delivery, and screening for diseases that are in their very early stages. Still a distant dream, significant progress in micro and nanotechnology brings us closer to materializing it. For such a miniature device to be injected into the body, it has to be 800 μm or smaller in diameter. Miniature, safe and energy efficient propulsion systems hold the key to maturing this technology but they pose significant challenges. Scaling the macroscale natation mechanisms to micro/nano length scales is unfeasible. It has been estimated that a vibrating-fin driven swimming robot shorter than 6 mm can not overcome the viscous drag forces in water. In this paper, the authors propose a new type of propulsion inspired by the motility mechanism of bacteria with peritrichous flagellation, such as *Escherichia coli*, *Salmonella typhimurium* and *Serratia marcescens*. The perfomance of the propulsive mechanism is estimated by modeling the dynamics of the motion. The motion of the moving organelle is simulated and key parameters such as velocity, distribution of force and power requirments for different configurations of the tail are determined theoretically. In order to validate the theoretical result, a scaled up model of the swimming robot is fabricated and characterized in silicone oil using the Buckingham PI theorem for scaling. The results are compared with the theoretically computed values. These robots are intended to swim in stagnation/low velocity biofluid and reach currently inaccessible areas of the human body for disease inspection and possibly treatment. Potential target regions to use these robots include eyeball cavity, cerebrospinal fluid and the urinary system.

Keywords: Swimming microrobot, biomimetic robotics, flagellar motion, resistive force theory, force characterization.

INTRODUCTION

Advent of microelectromechanical systems (MEMS) technology in 90's brought about the opportunity for miniaturizing the robots. Small scale swimming robots could be greatly beneficial for screening purposes in the fields of medical robotics and hydraulic systems. These smaller aquatic vessels will be able to reach and manipulate within regions traditionally inaccessible to larger devices.

Due to their small size, micro-swimming robots operate in very small Reynolds (Re) numbers. Reynolds number is defined as the ratio of inertia forces to viscous forces and characterizes fluid flow. A very low Reynolds number infers that inertial forces are negligible at microscale. Therefore, micro-swimming robots in general face challenges that larger scale swimming vehicles and robots do not.

Effective designs of small scale swimming robots have come from a variety of sources. One of the first micro-swimming robots was introduced by Fukuda *et al.* [1]. This robot, 50 mm in length and 6 mm in width, has a pair of fins and utilizes PiezoPZT($Pb(Zr,Ti)O_3$) for actuation. In order to enhance the effect of the resonance condition, it uses a magnification mechanism with magnification ratio of 326. Guo *et al.* [2] at Kagawa University in Japan have built a small scale swimming robot that has multiple degrees of freedom. This robot is 45mm long and 10 mm wide, and it is capable of controlling its depth, roll, and forward speed. The robot is propelled using ionic conductive polymer film (ICPF) actuators that produce undulatory motion, similar to the motion of a small fin. Two of these actuators work in tandem to power the robot. This robot was able to obtain speeds up to 5.5mm/s in experiments. There have been multiple variations or similar designs to the one above that use different actuation methods or have a different number of fins. Further miniaturization of the fish-like biomimetic devices will make them ineffective [1] because they rely on inertial forces for propulsion.

Another propulsion method, theorized by Ishiyama *et al*. [3], uses an external magnetic field to rotate a small screw in liquid. This magnetically operated micromachine does not require any power source or controller on the robot and it is not tethered. Hence, it is very attractive for medical surgery and catheter purposes. It has been demonstrated that this spiral type machine can swim in liquids of various viscosities in a broad range of Re numbers. Utilizing Buckingham PI's theorem, experiments were carried out on a millimeter sized machine in silicone oil with kinematic viscosity of $5x10^5$ mm^2/s. The Re number of this spiral machine was equal to that of a few micron size machine swimming in water. By applying magnetic fields of 100 Oe, it achieved the maximum linear velocity of 0.022 mm/s at 0.24 Hz frequency. For the frequency higher than the frequency which corresponds to the maximum speed, the rotation of the machine could not synchronize to the rotational frequency of the external field and the velocity decreased. Hence the frequency which yields the maximum speed is called the 'step-out' frequency. Magnetic Resonance Imaging (MRI) as a means for magnetic propulsion of a micromachine for MIS purposes has also been investigated at the University of Virginia [4] and Ecole Polytechnique de Montreal [5]. Besides the speed limitation issue, the key disadvantages of this robot are: (1) Patients with pacemakers, metal implants and bullet wounds can not be subjected to magnetic fields as magnetic forces might pull on these objects and damage healthy tissues. (2) Considering the low speed of the robot, the patient may be required to stay in the magnetic field for longer than the time allowed by FDA regulations (3) Magnetic gardient fields can produce eddy currents in the patient and cause local heating. This is not usually a concern in MRI, but it might become an issue if the robot is moving inside the body (4) Control and positioning of the magnetically propelled robot is another important unsolved problem [5].

Therefore, we propose a novel safe, miniature and energy efficient propulsion system potentially used on all patients with no restriction. Also, our design does not subject the patients to the discomfort of staying in magnetic field for an extended period of time.

Our proposed biomimetic propulsion concept is inspired by the peritrichous flagellation used by bacteria such as *E. Coli* and *S. Marcescens* [6]. The flagella of these cells are randomly distributed over the cell surface and each flagellar motor rotates independently of the others. Hydrodynamic interactions among flagella cause them to coalesce and bundle behind the cell during swimming [7]. *E.Coli* is a single celled organism that lives in aqueous environments. Depicted in Fig. 1, *E.Coli* cells are cylindrical rods with hemisphere ends. Flagellum is a propulsive organelle that includes a reversible rotary motor embedded in the cell wall, and a filament that extends into the external medium. The filament is a long (~ 10 µm), thin (~ 20nm) helix (2.5 µm pitch, 0.5 µm diameter) that turns at speed of ~100 Hz [8]. *E.coli*'s size and speed yields very low Reynolds number regime (Re=10^{-4}), where viscous effects are dominant and inertia forces are insignificant.

This research work intends to investigate the potential of using flagellar motion for microrobot propulsion. By spinning a rigidly fixed helical structure at low Reynolds numbers, a thrust force should be observed that can be used for propulsion of a micro swimmer. Increasing the number of these rigid helical structures (flagella) will increase the thrust force. Applying Buckingham PI theorem, a scaled-up model of the robot was constructed and tested in silicone oil. The resistive force theory model is used to predict the values for the thrust force and velocity of the robot. Experimental results are compared with predicted theoretical values.

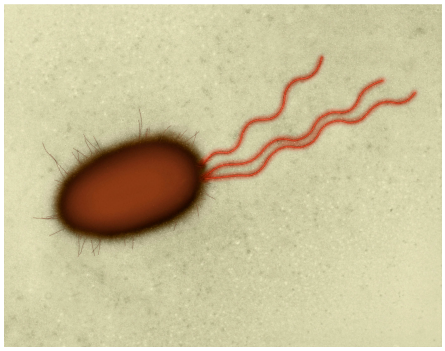

Fig.1. Transmission Electron Microscopy (TEM) image of *E. Coli* (x3515) "Image copyright Dennis Kunkel Microscopy, Inc. Used with permission"

NOMENCLATURE

A	Amplitude of the flagellum
C_D	Coefficient of drag of the head
$C_{D\Omega}$	Angular coefficient of drag of the head
C_l	Tangential coefficient of drag of the flagellum
C_n	Normal coefficient of drag of the flagellum
F_l	Tangential component of the force
F_n	Normal component of the force
F_x	Force in x direction
F_y	Force in y direction
b	Half of the thickness of the flagellum
L	The length of the flagellum
Re	Reynolds number
U	Axial velocity of the robot
l	Characteristic dimension of the object
p	Pressure
λ	Wavelength of the flagellum
μ	Dynamic viscosity of the fluid
ρ	Density of the fluid
θ	Angle between basal end of the flagellum and x axis
Ω	Angular velocity of the head
Subscripts:	
x	Subscript for components in x direction
y	Subscript for components in y direction
n	Subscript for normal components
l	Subscript for lateral components

MODELING

A. Low Reynolds Number Flow

Reynolds number is defined as:

$$Re = \frac{\rho V l}{\mu} \tag{1}$$

where ρ and μ are density and dynamic viscosity of the fluid, respectively. V is the flow velocity and l is the characteristic dimension of the object. For the microscale objects moving in water, due to the size of the object and fluid properties of water, $Re<<1$. This type flow is known as Stokes or stagnation flow. For this type of flow Navier-Stokes equation reduces to:

$$\nabla p + \mu \nabla^2 U = 0 \tag{2}$$

where p is the pressure and U is the velocity. This equation is absent of any time dependent terms, signifying that the generated propulsion force only depends on the propeller's position. This infers any motion that completely retraces its own steps, like the flapping of fish's tail, will result in no net forward movement. The classic example is the motion of scallop. Scallop propels forward by slowly opening its hinge and then quickly closing it; if scallop were scaled down to be a few microns, this motion would result in periodic slight forward and backward motion of the exact same amount.

To overcome this problem, organisms living in low Reynolds number regimes have developed moving organelles which have a *handedness* to them. For instance, *E. Coli*'s flagella rotate with a helical motion, much like a corkscrew. This configuration produces patterns of motion that do not repeat the first half of the cycle in reverse for the second half, allowing the organisms to achieve movement in their environment.

B. Modeling of the flagellar motion

Due to complex nature of the motion, flagellar motion is very difficult to model. Nonetheless, multiple methods of analyzing the resultant force of rotating flagella or similar structures have been developed.

In 1955, Gray and Hancock [9] used the slenderness of flagellum and related the local drag force of every point along the flagellum to its corresponding local velocity. They assumed that normal, binormal and tangential components of drag force are proportional to the respective component of the velocity with different proportionality constants. Several modifications to the Gray and Hancock theory were developed. These modified models had more accurate empirical equations for the drag coefficients. In general, this approach is known as resistive force theory (RFT). RFT does not yield accurate results when the moving organelle is attached to the cell body. Also, it is not applicable to the multi-flagella case due to the fact that the empirical coefficients are calculated for the single flagellum case.

Regardless of the inadequacies of the RFT, it is a robust method to start with. Figure 2 shows a simple schematic of the proposed micro-swimming robot. Equation (2) indicates that the motion is non-accelerating. Therefore, equations for conservation of force and momentum simplify to the following equations:

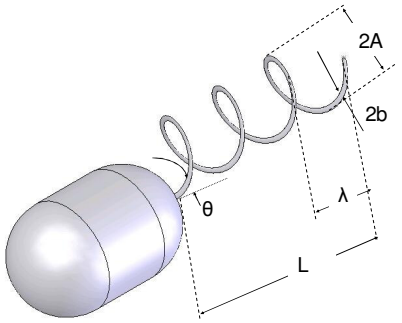

Fig. 2. Schematic of the swimming microrobot propelled by flagellar motion

$$\begin{aligned} LF_x + C_D U &= 0 \\ ALF_y + C_{D\Omega}\Omega &= 0 \end{aligned} \tag{3}$$

where F_x and F_y are forces in x and y directions. C_D and $C_{D\Omega}$ are respectively coefficient of drag and angular coefficient of drag of the head. L is the length of the flagellum and A is the amplitude. U is the axial velocity of the robot and Ω is the angular velocity of the head. The forces in x and y direction can then be written in the normal and tangential components:

$$\begin{aligned} F_x &= F_l \cos\theta - F_n \sin\theta \\ F_y &= F_l \sin\theta + F_n \cos\theta \end{aligned} \tag{4}$$

in which θ is defined by:

$$\tan\theta = \frac{\lambda}{2\pi A} \tag{5}$$

where λ is the wavelength of the tail. According to the RFT model [9], normal and tangential forces can be written as:

$$\begin{aligned} F_l &= -C_l (U\cos\theta - \omega A \sin\theta) \\ F_n &= -C_n (-U\sin\theta - \omega A \cos\theta) \end{aligned} \tag{6}$$

where:

$$\begin{aligned} C_l &= \frac{2\pi\mu}{\ln(\frac{2\lambda}{b}) - \frac{1}{2}} \\ C_n &= \frac{4\pi\mu}{\ln(\frac{2\lambda}{b}) + \frac{1}{2}} \end{aligned} \tag{7}$$

and ω is the angular velocity of the tail. Coefficients C_l and C_n are empirically derived for a single flagellum with both free ends. Using these coefficients for the case in which flagellum is attached to a body will result in overestimation the thrust force.

Figure 3 shows predicted values for thrust force as a function of θ for different values of flagellum angular velocity, ω. The dimensions of the robot used in the RFT model are included in Table 1. In our particular experimental setup, explained in the following section, the robot is fixed to a beam, therefore $U = 0$. This will result in decrement of the drag force.

To simplify the fabrication and characterization process, utilizing the Buckingham PI theorem, the dimensions of the robot are scaled up and to compensate for that, the experiment is performed in silicone oil which is about 30 times more

viscous than water. According to Buckingham PI theorem, the ratio of $\frac{F_x}{\rho V^2 D^2}$ scaled up model produces the same amount of thrust force as the miniature robot does [10].

EXPERIMENTAL SETUP

In order to examine the theory of flagellar propulsion for a microrobot, an experimental setup was constructed to measure the thrust force which is produced from the rotation of a helical tail at Reynolds numbers comparable to those of microorganisms. Components of the setup are described below.

A. *Flagellum and Motor*

A flagellum and a rotary actuator are two essential elements required for replication of the flagellar motion. In order to create the tail, a metallic spring with 260 µm wire diameter and 6.6 mm helical diameter was stretched to 8.8 mm pitch and 2.3 cm length. This *flagellum* was then attached to the rotary actuator with superglue.

The actuator used was a Myonic Smoovy® motor. The Smoovy motor is a DC brushless motor measuring just under 13 mm long and has a body diameter of 5mm and a shaft diameter of 1mm. The Smoovy motor can run at variable frequencies ranging from 1 to 15,000 RPM [10]. Smoovy's small size and variable speed control made it a perfect choice for actuation. Furthermore, the Smoovy can run fully submerged in liquid, which is also important for this particular application. Smoovy's speed is controlled through a control board which is configured from a data acquisition board.

Table 1: Dimension of the swimming microrobot

Half of the thickness of the flagellum, b	23 µm
Amplitude of the flagellum, A	3.3 mm
Wavelength of the flagellum, λ	3.8 mm
Length of the flagellum, L	2.3 cm

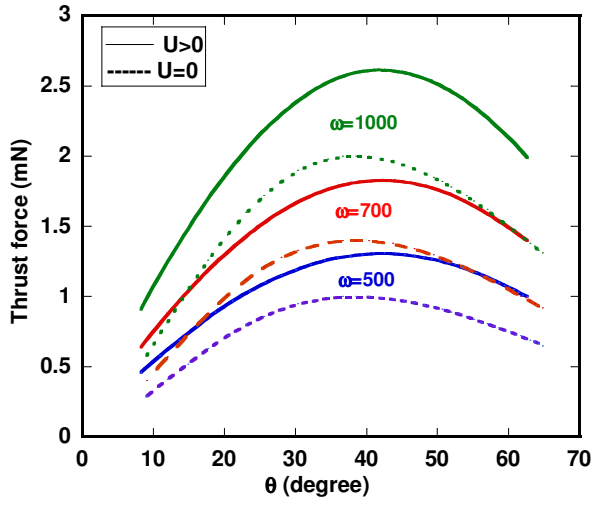

Fig 3. Thrust force as a function of θ for different angular velocity of the flagellum

B. *Force Sensor*

In order to sense the thrust force created by the rotation of the flagellum, a force characterization system was developed. The Smoovy motor was perpendicularly mounted to a very thin cantilever beam, which is 13 cm long and has a square cross section of 1.6x1.6 mm^2. At the top of the beam, two Entran® semiconductor strain gages were attached. The rotation of the flagellum creates a thrust force in the oil which deflects the beam, straining the strain gages and causing a change in the voltage drop across them, and this change in voltage can be used to measure the thrust force.

The force characterization system is depicted in Fig. 4. Essentially, it was ensured that the Smoovy motor is fully submerged in the oil and sufficiently far away from the bottom of the tank so that there is no wall effect.

The force sensor circuit is composed of a Wheatstone bridge circuit and a differential amplifier. In order to stabilize the output voltage, two voltage followers were used before the differential amplifier. In the case of our particular system, the strain gages had a resistance of ~360 Ohms, one of the two other resistors of the bridge had a resistance of ~320 Ohms, and the last resistor in the Wheatstone bridge was made variable so that the zero value of the bridge when no load was applied could be adjusted.

A CA-1000 National Instruments Data Acquisition Board (DAQ) reads the voltage output of the amplifying circuit into the MATLAB® program at a sample rate of 1 KHz over 10 seconds. The raw data taken from the DAQ was passed through a Butterworth filter to eliminate the noise.

The system was calibrated and sensitivity of the sensing bar was determined before experiments. In order to calibrate the force sensor, the rig was placed on its side and an increasing amount of weight was placed on the free end of the beam. The output voltage for each weight was recorded as well as the zero value when no weight was applied. A graph of weight vs. output voltage was then created and a linear fit was made to the data. To measure the sensitivity of the setup, a weight would

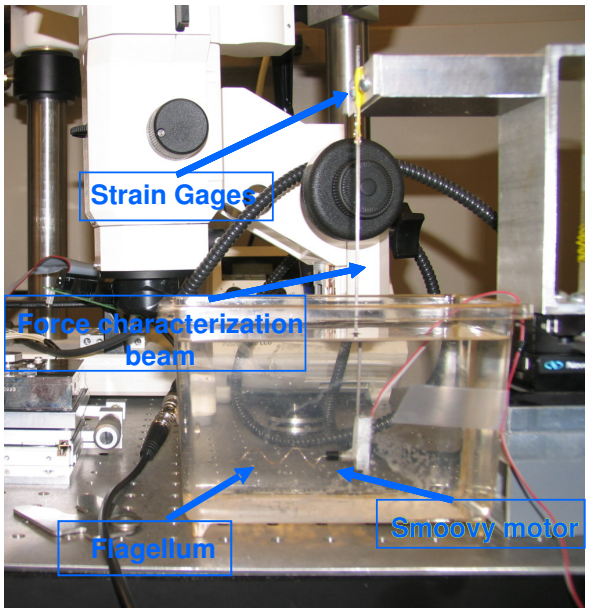

Fig. 4. Force measurement system

be tested several times on the bar and the difference between the predicted output voltage from the calibration and the actual output voltage was recorded. Sensitivity of the bar was calculated to be 1 mN.

Once calibration and sensitivity measurements were taken, the scaled up model was attached to the force sensing bar and then placed into a container of Dow Corning 200® Fluid, 350 cst. The motor was set to rotate at a given frequency and allowed time to reach a steady state condition in the oil. The MATLAB program was then used to record the voltage being outputted by the amplifying circuit.

EXPERIMENTAL RESULTS

Results of the experiment are depicted in Fig. 5. Theoretical values for the thrust force predicted by RFT overestimated the experimental values of force by a constant factor. There are several reasons for this:

- Empirical coefficients, C_l and C_n, are for a flagellum swimming with both ends free. In this experiment one end of the flagellum was connected to the shaft which results in a decrease in thrust force
- Fabricated flagellum lacks consistency in pitch diameter and wavelength which further effects the drag coefficients.
- Due to the resistance of the highly viscous silicone oil, flagellum is rotating at frequencies smaller than the nominal frequency which causes a decrease in thrust force.
- Due to small size of the motor shaft, the flagellum could not be attached completely concentric with the shaft of the motor; therefore the resultant force was less than the theoretically predicted value.

All the aforementioned sources of decrease in thrust force are approximately constant regardless of the frequency that the motor is running at. Therefore, as it is seen in Fig. 5 thrust force is underestimated by a constant amount.

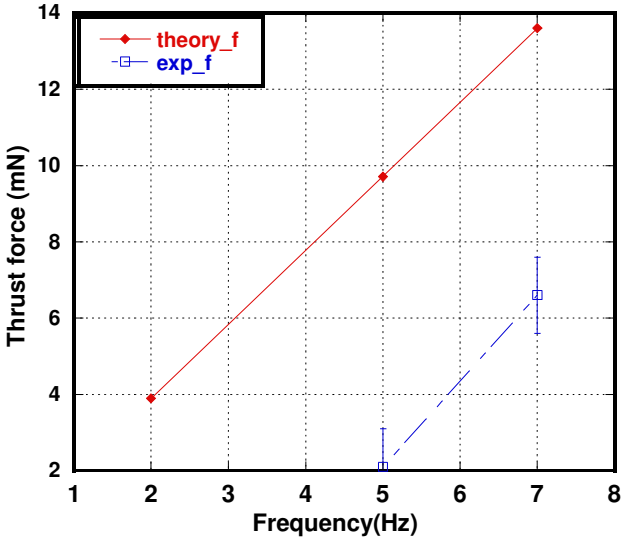

Fig. 5. Thrust force as a function of frequency

CONCLUSIONS

A new biomimetic propulsion mechanism inspired by flagellar motion of bacteria is introduced. RFT model is used to predict the values for thrust force of the robot. Applying Buckingham Pi theorem a scaled-up model of the robot was constructed and tested in silicone oil which is 30 times more viscous than water. Preliminary experimental results for thrust force are shown to be overestimated by the RFT model by a constant amount for all frequencies. Possible reasons causing this discrepancy are outlined. This experiment proves the proposed concept. As future work, more experiments will be conducted by varying tail and body parameters, the finite element analysis of the body propulsion forces by incorporating the multiple tail coupling effects will be conducted, and the swimming robot system will be miniaturized. As a target medical application, the developed swimming robot will be used for diagnosis and drug delivery in steady-state flow liquid environments inside the human body such as the urinary system.

ACKNOWLEDGMENTS

Authors thank their colleagues specially Gordon Christopher, Gaurav Shah and Carlo Menon from the NanoRobotics laboratory at Carnegie Mellon University for stimulating discussions. They also thank Chytra Pawashe for helping with control and data acquisition from the motor.

REFERENCES

[1] Fukuda, T., Kawamoto, A., Arai, F. and Matsuura, H., 1994, "Mechanism and Swimming Experiment of Micro Mobile Robot in Water," *Proc. of IEEE Int'l Workshop on Micro Electro Mechanical Systems (MEMS'94),* pp.273-278.

[2] Guo, S., Hasegaw, Y., Fukuda, T., and Asaka, K., 2001, "Fish –Like Underwater Microrobot with Multi DOF," *Proceedings of 200 International Symposium on Micromechatronics and Human Science*, pp. 63-68.

[3] Honda, T., Arai, K. and Ishiyama, K., 1999, "Effect of Micro Machine Shape on Swimming Properties of the Spiral-Type Magnetic Micro-Machine," *IEEE transaction on magnetics*, **35**, pp. 3688-3690.

[4] McNeil, R., Ritter, R., Wang, B., Lawson, M., Gillies, G., Wika, K., Quate, E., Howard, M., and Grady, M., 1995 "Functional Design Features and Initial Performance Characteristics of a Magnetic-Implant Guidance System for Stereotactic Neurosurgery," *IEEE Transaction on Biomedical Engineering*, **42**, pp. 793-801.

[5] Mathieu J.B., Martel S., Yahia L., Soulez G., and Beaudoin G., 2003, "MRI Systems as a Mean of Propulsion for a Microdevice in Blood Vessels," *Proceedings of the 25th Annual International Conference of the IEEE Engineering in Medicine and Biology Conference*.

[6] Edd, J., Payen, S., Rubinsky, B., Stoller, M.L. and Sitti, M., 2003, "Biomimetic Propulsion for a Swimming Surgical Microrobot," *Proceedings of the 2003 IEEE/RSJ*, pp. 2583-2588.

[7] Darnton, N., Turner, L., Breuer, K., and Berg, H., "Moving Fluid with Bacterial Carpets," *Biophyiscal Journal*, **86**, pp. 1863-1870, March 2004.

[8] Leifson, E., 1960 "Atlas of Bacterial Flagellation," *Academic Press, New York and London*..

[9] Gray, J. and Hancock, G., 1955, "The Propulsion of Sea-Urchin Spermatoza," *Journal of Experimental Biology*, **32**, pp. 802-814.

[10] Fox, R., McDonald, A., and Pritchard, P., 2004, "Introduction to Fluid Mechanics," John Wiely & Sons, pp. 273-300.

[11] http://www.mpsag.com/